HHS Public Access

Author manuscript

Brain. Author manuscript; available in PMC 2015 June 03.

Published in final edited form as:

Brain. 2007 July ; 130(0 7): 1834–1846. doi:10.1093/brain/awm086.

Changes in network activity with the progression of Parkinson's disease

Chaorui Huang[1,2], **Chengke Tang**[1,2], **Andrew Feigin**[1,2], **Martin Lesser**[3], **Yilong Ma**[1,2], **Michael Pourfar**[1,2], **Vijay Dhawan**[1,2], and **David Eidelberg**[1,2]

[1]Center for Neurosciences, The Feinstein Institute for Medical Research, North Shore-Long Island Jewish Health System, Manhasset, NY

[2]Departments of Neurology and Medicine, North Shore University Hospital and New York University School of Medicine, New York, NY

[3]Biostatistics Unit, The Feinstein Institute for Medical Research, North Shore-Long Island Jewish Health System, Manhasset, NY, USA

Abstract

Parkinson's disease (PD) is associated with abnormal activity in spatially distributed neural systems mediating the motor and cognitive manifestations of this disorder. Metabolic PET studies have demonstrated that this illness is characterized by a set of reproducible functional brain networks that correlate with these clinical features. The time at which these abnormalities appear is unknown, as is their relationship to concurrent clinical and dopaminergic indices of disease progression.

In this longitudinal study, 15 early stage PD patients (age 58.0 ± 10.2 years; Hoehn and Yahr Stage 1.2 ± 0.3) were enrolled within 2 years of diagnosis. The subjects underwent multitracer PET imaging at baseline, 24 and 48 months. At each timepoint they were scanned with [^{18}F]-fluorodeoxyglucose (FDG) to assess longitudinal changes in regional glucose utilization and in the expression of the PD-related motor (PDRP) and cognitive metabolic covariance patterns (PDCP). At each timepoint the subjects also underwent PET imaging with [^{18}F]-fluoropropyl βCIT (FP-CIT) to quantify longitudinal changes in caudate and putamen dopamine transporter (DAT) binding. Regional metabolic changes across the three timepoints were localized using statistical parametric mapping (SPM). Longitudinal changes in regional metabolism and network activity, caudate/putamen DAT binding, and Unified Parkinson's Disease Rating Scale (UPDRS) motor ratings were assessed using repeated measures analysis of variance (RMANOVA). Relationships between these measures of disease progression were assessed by computing within-subject correlation coefficients.

We found that disease progression was associated with increasing metabolism in the subthalamic nucleus (STN) and internal globus pallidus (GPi) (P<0.001), as well as in the dorsal pons and primary motor cortex (P<0.0001). Advancing disease was also associated with declining

Correspondence to: David Eidelberg, MD, Center for Neurosciences, Feinstein Institute for Medical Research, North Shore-Long Island Jewish Health System, 350 Community Drive, Manhasset, NY 11030, USA, david1@nshs.edu.

metabolism in the prefrontal and inferior parietal regions ($P<0.001$). PDRP expression was elevated at baseline relative to healthy control subjects ($P<0.04$), and increased progressively over time ($P<0.0001$). PDCP activity also increased with time ($P<0.0001$). However, these changes in network activity were slower than for the PDRP ($P<0.04$), reaching abnormal levels only at the final timepoint. Changes in PDRP activity, but not PDCP activity, correlated with concurrent declines in striatal DAT binding ($P<0.01$) and increases in motor ratings ($P<0.005$). Significant within-subject correlations ($P<0.01$) were also evident between the latter two progression indices.

The early stages of PD are associated with progressive increases and decreases in regional metabolism at key nodes of the motor and cognitive networks that characterize the illness. Potential disease-modifying therapies may alter the time course of one or both of these abnormal networks.

Keywords

Parkinson's disease; PET; ^{18}F-fluorodeoxyglucose (FDG); glucose metabolism; network analysis

Introduction

Accurate and comprehensive descriptions of the natural history of Parkinson's disease (PD) are critical to the assessment of new therapies for this disorder. Knowledge of the rate of disease progression, particularly at early phases of the illness, is essential for the design of clinical trials aimed at evaluating potential neuroprotective treatment strategies. However, such determinations can be difficult when based solely upon clinical assessments, especially if different manifestations of disease do not evolve in parallel. For instance, the rate of progression in standardized clinical ratings is different for PD patients with tremor- and gait-predominant presentations (Jankovic and Kapadia, 2001). These subpopulations also appear to differ in their propensity to develop cognitive impairment (Zetusky *et al*., 1985; Alves *et al*., 2006). Additionally, the rate of progression for a given clino-pathological feature may not be constant. Indeed, this phenomenon has been observed in PD, with accelerated nigral dopamine loss at early stages of the disease (Fearnley and Lees, 1991; cf. Morrish *et al*., 1998; Hilker *et al*., 2003). Furthermore, at a specific clinical stage, progression can vary across individual subjects depending upon demographic factors such as age of onset (cf. Nakamura *et al*., 2001; Alves *et al*., 2005). The observed rate of clinical deterioration can also be affected by concurrent symptomatic therapy, especially when the effects of treatment are long lasting (Fahn *et al*., 2004).

Because of these considerations, attention has turned toward the use of imaging biomarkers as a potentially more objective and accurate means of gauging disease progression (see e.g. Brooks *et al*., 2003; Au *et al*., 2005 for reviews). Radiotracer-based imaging assessments of presynaptic nigrostriatal dopaminergic functioning have been included in several recent clinical trials designed to evaluate disease modifying therapies (Marek *et al*., 2003; Whone *et al*., 2003; Fahn *et al*., 2004). However, the conflicting nature of the findings has suggested a complex relationship between the clinical and imaging-based measures (Ravina *et al*., 2005). Furthermore, while suitable for the *in vivo* assessment of nigrostriatal function, these

radiotracer approaches are not designed to capture the effects of disease on physiologically relevant neural systems, including non-dopaminergic pathways.

Other imaging strategies can be used to assess changes in brain function with advancing disease. Network analysis has been used extensively with metabolic imaging to study the pathophysiology of parkinsonism and its treatment (e.g. Asanuma *et al*., 2006; Trošt *et al*., 2006; for reviews see Carbon *et al*., 2003*a*; Eckert and Eidelberg, 2005). The motor features of PD are associated with the expression of an abnormal metabolic pattern characterized by increased pallidothalamic and pontine activity, associated with relative reductions in cortical motor regions (Eidelberg *et al*., 1994; 1997; cf. Carbon *et al*., 2003*a*). This PD-related spatial covariance pattern (PDRP) has thus far been detected in eight independent patient populations (Moeller *et al*., 1999; Feigin *et al*., 2002; Lozza *et al*., 2004; Asanuma *et al*., 2005; Eckert *et al*., 2007). Moreover, we have recently demonstrated that PDRP expression is highly reproducible in individual subjects, with stable network activity over hours to weeks (Ma *et al*., 2007). In addition to providing accurate discrimination between PD patients and controls (Asanuma *et al*., 2005; Eckert *et al*., 2007; Ma *et al*., 2007), PDRP expression has been found consistently to correlate with standardized motor ratings (Lozza *et al*., 2004; Asanuma *et al*., 2006; cf. Eidelberg *et al*., 1994, 1995) as well as with symptom duration (Moeller and Eidelberg, 1997). Thus, this measure of pathological network activity can provide a useful quantitative descriptor of advancing motor dysfunction in PD.

Network analysis has also provided unique insights into the mechanisms underlying abnormal cognitive functioning in PD. In a study of regional glucose metabolism in non-demented patients, we used a covariance mapping approach to identify a significant pattern associated with executive dysfunction (Mentis *et al*., 2002). These FDG PET data were the basis for a recent comprehensive spatial covariance analysis in which neuropsychological performance in PD patients was found to be correlated with the activity of a distinct metabolic network that was topographically unrelated to the PDRP (Huang *et al*., 2007; cf. Lozza *et al*., 2004). This PD-related cognitive pattern (PDCP) was characterized by reduced metabolic activity in prefrontal and parietal cortex, associated with relative increases in the cerebellum and dentate nuclei. PDCP expression in individual patients correlated consistently with performance on tests of memory and executive function and has recently been found to be elevated in PD patients with neuropsychologically defined criteria for minimal cognitive impairment (Huang *et al*., in press). These network values were also found to be highly reproducible over an 8-week period and were not altered by routine antiparkinsonian therapies such as levodopa or subthalamic nucleus (STN) deep brain stimulation (Huang *et al*., 2007; cf. Asanuma *et al*., 2006). These findings suggest that this network may have utility as an objective biomarker of cognitive functioning at early clinical stages of the disease.

Although substantial information exists linking these metabolic networks to the motor and cognitive manifestations of PD, little is known about the actual time course of their evolution during the early phases of the illness. In this regard, it would be useful to measure the rate at which their expression changes with time, as well as to examine the relationship between these changes and concurrent clinical and dopaminergic imaging measures of

disease progression. To address these issues, we performed a longitudinal multi-tracer PET imaging study of early stage PD patients followed over a 4-year period.

Material and Methods

Subjects

Fifteen right-handed PD patients [11 males and 4 females, age: 58.0 ± 10.2 years (mean ± SD)] participated in this longitudinal study. A diagnosis of PD was made according to the UK Brain Bank criteria (Hughes *et al*., 1992); patients were enrolled within 2 years of diagnosis. At baseline, the patients had predominantly unilateral motor signs (Hoehn and Yahr Stage: 1.2 ± 0.3, mean ± SD). Nine patients had predominant right-sided limb involvement; the remaining six had predominant involvement of the left limbs. Clinical and imaging evaluations were conducted at the first visit and were repeated approximately 2 years later (mean interval 2.1 ± 0.6 years). Ten of the participants returned for further assessment at a third timepoint approximately 4 years from baseline (mean interval 3.9 ± 0.7 years). Of the five subjects who did not return for the final timepoint, three relocated and two refused to participate in further testing.

Of the 15 original subjects, eight were drug-naïve at baseline; the remaining seven patients were chronically treated with anti-parkinsonian medication at the time of enrollment. The medicated patients were on levodopa singly (n = 1), levodopa in combination with selegiline and/or dopamine agonists (n = 3), or on mono-therapy with either selegiline (n = 1) or dopamine agonists (n = 2). Seven of the initially unmedicated patients required treatment by the second timepoint, receiving either levodopa (n = 3) or dopamine agonists (n = 4). By the third timepoint, all participants required levodopa singly or in combination with a dopamine agonist.

Positron emission tomography

At each timepoint, subjects underwent PET imaging with ^{18}F-fluorodeoxyglucose (FDG) to quantify regional glucose metabolism and ^{18}F-fluoropropyl βCIT (FPCIT) to measure caudate and putamen dopamine transporter (DAT) binding (Kazumata *et al*., 1998; Ma *et al*., 2002). At each timepoint, the two scans were separated by an average interval of approximately 3 weeks (mean interval: 27, 16 and 13 days for the three timepoints, respectively). They fasted overnight before each imaging session; all antiparkinsonian medications were held for at least 12 h before the PET procedures. The subjects were evaluated according to the Unified Parkinson's Disease Rating Scale (UPDRS, Fahn *et al*., 1987) immediately prior to imaging.

PET imaging was performed in 3D mode using a GE Advance tomograph (General Electric; Milwaukee, WI, USA). The 18-ring bismuth germanate scanner provide 35 image planes with an axial field of view of 14.5 cm and an intrinsic resolution of 4.2 mm (FWHM) in all directions. PET scans were conducted in a dimly lit room with minimal auditory stimulation with eyes open. Patients were positioned in the scanner using a stereoadapter with 3D laser alignment with reference to the orbitomeatal line; identical stereoadapter and laser settings were used in each imaging session. Ethical permission for these procedures was obtained

from the Institute Review Board of North Shore University Hospital. Written consent was obtained from each subject with detailed explanation of the procedures.

Data analysis

Striatal DAT binding—The FPCIT PET scans from each subject were realigned to the image frame acquired at 40 min post injection to correct for possible motion artefact (Ma *et al*., 2002). Regions-of-interest (ROIs) were placed on the caudate and putamen bilaterally and on the occipital cortex (Carbon *et al*., 2004). The ROIs were defined on a single slice summed over the striatal sections and were individually adjusted for each subject. All three scans were realigned to the baseline scan so that the same ROI template was used across the three timepoints. At each timepoint, caudate and putamen DAT binding was estimated for each hemisphere by the striatal-to-occipital ratio (SOR), defined as (striatum –-occipital)/ occipital counts in a single 10 min frame beginning at 90 min after the tracer injection (Kazumata *et al*., 1998; Ma *et al*., 2002). These values were averaged across hemispheres and compared with analogous values from 10 healthy volunteers (4 males and 6 females; age 60.0 ± 9.9 years).

Regional glucose metabolism—Regional and global rates of glucose metabolism were computed on a voxel basis for each FDG PET scan utilizing a single arterial sampling method (Takikawa *et al*., 1993). The metabolic images were then processed using SPM99 (Wellcome Department of Cognitive Neurology, Institute of Neurology, London) running on Matlab 6.5 (Mathworks, Inc., Natick, MA). The scans from each subject were realigned and spatially normalized to a Talairach-based FDG PET template. The normalized data were then smoothed using a Gaussian kernel at FWHM = 10 mm. Global normalization was performed using proportional scaling.

Longitudinal changes in regional metabolism for the entire cohort (n = 15) were assessed across the three timepoints using the ‘multisubjects, conditions and covariates’ model in SPM. Contrasts defined as ‘−1 0.5 0.5’ and ‘1 −0.5 −0.5’ were used to assess increasing and decreasing brain metabolism over time, respectively. Changes were considered significant at a threshold of P<0.05 corrected at the cluster level, as well as at a false discovery rate (FDR)-corrected threshold of P<0.05 at the voxel level. Coordinates were reported in the standard anatomical space developed at the Montreal Neurological Institute. The localization of each reported cluster was confirmed using the Talairach space utility (available at http://www.ihb.spb.ru/~pet_lab/TSU/TSUMain.html). We used the atlas of Schmahmann (2000) to localize clusters within the cerebellum and related structures.

For each significant cluster, we performed a *post hoc* analysis in which metabolic activity at each timepoint was measured within a sphere (radius = 4 mm) centred on the peak voxel. Each regional value was ratio normalized by the global metabolic rate measured in that scan. These measures were then adjusted to the group mean by multiplication with the average global value across subjects. The data were plotted and displayed with respect to reference values from 15 healthy volunteer subjects (8 males and 7 females; age 56.7 ± 12.3 years).

Network analysis

Using a network quantification approach (Ma *et al*., 2007; Spetsieris *et al*., 2006), we assessed longitudinal changes in the expression of the two disease-related spatial covariance patterns that we had previously identified and validated in the metabolic data of PD patients. The first pattern was identified during a voxel-driven principal components analysis (PCA) of FDG PET scans from a combined group of PD patients and age-matched healthy volunteers (Ma *et al*., 2007). This PD-related motor pattern (PDRP; Fig. 1A) was characterized by increased pallidothalamic and pontine metabolic activity associated with relative metabolic reductions in the premotor and supplementary motor areas and parieto-occipital association regions. We have recently described a separate spatial covariance pattern that is associated with memory and executive functioning in non-demented PD patients (Huang *et al*., 2007). This PD-related cognitive pattern (PDCP; Fig. 1B) was characterized by reductions in prefrontal and parietal metabolism associated with relative increases in the cerebellum and dentate nuclei.

In all subjects, the expression of the PDRP and PDCP networks was separately quantified at each timepoint using a fully automated voxel-based algorithm (software available at http://neuroscience-nslij.org/Methods/software.html, Spetsieris *et al*., 2006; Ma *et al*., 2007). All network computations were performed blind to subject, timepoint (0, 24 or 48 months), baseline treatment status (drug naïve or initially treated) and disease severity (UPDRS motor ratings). Reference values for PDRP and PDCP expression were computed in the same group of 15 age-matched healthy volunteer subjects that was used for the *post hoc* analysis of the SPM results (see earlier). Subject scores for the entire cohort (PD patients and healthy controls) were *z*-transformed and offset so that the control mean was zero.

Statistical analysis

PDRP and PDCP scores computed in the baseline scans ($n = 15$) were separately compared with control values using two-tailed Student's *t*-tests. One-way repeated measure analysis of variance (RMANOVA) was performed on the data of all 15 subjects acquired at the three timepoints to evaluate longitudinal changes in UPDRS motor ratings, mean left–right caudate/putamen DAT binding, regional metabolic measures and PDRP/PDCP network activity. These analyses were performed using an iterative method to fit a mixed model for each RMANOVA (Searle *et al*., 1992). This approach allowed for the inclusion of subjects with missing data to provide a more precise and reliable estimation of the data at each timepoint, thereby increasing the power of the whole model (cf. Ellis *et al*., 2000). *Post hoc* comparisons were performed between timepoints (e.g. 2–1, 3–2, 3–1) using Tukey's HSD tests. To examine the effects of initial medication status on baseline motor ratings, striatal DAT binding and network expression, we compared these measures in the drug-naïve and initially medicated subgroups. We also determined whether progression rates for each of these measures differed for these two subgroups. This was accomplished by using a two-way RMANOVA that included initial medication status as the between-subject variable and timepoints as the repeated within-subject variable.

The degree of linearity in the changes in the clinical, dopaminergic imaging and network measures with disease progression was assessed by fitting a simple linear regression model

to the data from the 10 participants who were scanned at all three timepoints. R^2 values were computed by regression for each subject; the mean value was used to represent the overall linearity of change in each measure over time. If linearity was evident (i.e. mean R^2>0.9), the annual rate of change for each individual was computed by dividing the difference in the measure between timepoints 1 and 3 by the corresponding time interval. The mean rate of change across subjects was used to represent the rate of change per year for the PD group. Additionally, we used the Wilcoxon signed rank test to compare the R^2 values for the PDRP and PDCP scores as a means of assessing the relative linearity of the trajectories of the two measures.

Lastly, we computed within-subject correlation coefficients (Bland and Altman, 1995) to determine the relationship between changes in the clinical and imaging progression indices over the three longitudinal timepoints. For all analyses, the significance level was set at P<0.05. Statistical analyses were performed using SAS 9.1 (SAS Institute Inc.).

Results

Clinical ratings

Off-state UPDRS motor ratings at the three timepoints are presented in Fig. 2. These values increased significantly over time [F(2,17) = 23.2, P<0.0001; RMANOVA]. *Post hoc* testing with respect to baseline revealed significant increases in motor ratings at both the second (P<0.001) and third timepoints (P<0.0001), with a trend toward an increase between these timepoints (P = 0.08). Overall, the increase in UPDRS motor ratings was linear over time (mean R^2 = 0.91), with an average rate of 2.1 points per year.

Striatal DAT binding

Caudate and putamen DAT binding values at the three timepoints are presented in Table 1 and Fig. 3. At baseline, DAT binding was 97.3% (P = 0.79) and 54.7% (P<0.001) of the normal mean for the caudate and putamen, respectively. DAT binding for the two measures fell to 88.5% (P = 0.21) and 48.1% (P<0.001) of normal at 24 months, and 77.4% (P<0.02) and 40.0% (P<0.001) at 48 months. These measures declined significantly over time [caudate: F(2,17) = 10.2; putamen: F(2,17) = 8.4, P<0.003; RMANOVA]. *Post hoc* testing revealed significant reductions in DAT binding at the third timepoint relative to baseline (caudate: P<0.001; putamen: P<0.005), with a trend toward decline at the second timepoint (caudate: P = 0.06; putamen: P = 0.07). Declines in striatal DAT binding between the second and third timepoints were not significant (caudate: P = 0.12; putamen: P = 0.23).

The decline in caudate and putamen DAT binding was linear (mean R^2 = 0.94 for both regions), corresponding to an average rate of 5.2 and 3.9% of normal per year for the two regions, respectively. Declines for the caudate and putamen were highly intercorrelated (r = 0.91, P<0.0001), and both correlated with concurrent increases in UPDRS motor ratings (caudate: r = −0.60, P<0.01; putamen: r = −0.59, P<0.01).

Regional glucose metabolism

Global rates of glucose metabolism in the PD patients did not differ from normal (P>0.3) at any of the three timepoints (PD: 7.31 ± 1.55, 6.91 ± 1.32, 6.40 ± 1.90 mg/min/100 g at baseline, 24 months and 48 months; normal: 7.03 ± 1.38 mg/min/100 g). These measures did not change significantly over the 4-year period of follow-up [$F(2,23) = 0.9$, $P = 0.44$; RMANOVA]. Regions with significant metabolic changes over time are presented in Table 2 and Fig. 4. Progressive metabolic increases (P<0.001; Fig. 4A, *top*) were detected in the left STN, and in the right internal globus pallidus (GPi) and the adjacent subthalamic region. Continuous increases (P<0.0001) were also present in the dorsal pons, in the vicinity of the pedunculopontine nucleus (PPN) and the adjacent cerebellar hemisphere. Additionally, regional metabolism in the left primary motor cortex and the adjacent supplementary motor area (SMA) increased between the first and second timepoints, remaining stable throughout the rest of the follow-up period. At baseline, significant elevations relative to controls were present only in the dorsal pontine region (P<0.05). Regional metabolism in the GPi and motor cortex reached abnormal levels (P<0.05 and P<0.01, respectively) at the second timepoint. All the increasing regions, including the STN, attained supernormal levels of metabolic activity (P<0.01) by the final timepoint.

Declines in regional metabolism with advancing disease (P<0.001; Fig. 4A, *bottom*) were present bilaterally in the prefrontal region (BA 9/10) and in the inferior parietal lobule (BA 40). Despite the highly significant decline in the former region, local metabolic activity did not fall to subnormal levels during the course of the study. In the latter region, metabolic reductions reached significance (P<0.05) only at the final timepoint. Although all the reported regions exhibiting longitudinal change (Table 2) were localized to a single hemisphere, in each case significant metabolic progression (P<0.005) was noted in homologous areas of the opposite hemisphere.

Network analysis

Mean values for PDRP and PDCP expression at the three timepoints are displayed in Fig. 5. At baseline, PDRP expression was significantly higher in the PD patients relative to controls ($t = 2.24$; P<0.04), whereas PDCP expression did not differ across the two groups ($t = 0.75$; $P = 0.46$). Both networks exhibited significant changes in activity over time [PDRP: $F(2,23) = 29.9$, PDCP: $F(2,23) = 15.3$; P<0.0001 for both networks; RMANOVA]. *Post hoc* testing revealed an increase in PDRP expression from baseline to the second (P<0.05) and third timepoints (P<0.0001), and between the second and third timepoints (P<0.0001). In contrast, PDCP expression did not change between baseline and the second timepoint ($P = 0.31$), but was elevated at the third timepoint with respect to baseline and second timepoint values P<0.005), and with respect to healthy control values (P<0.001).

Although a significant correlation was noted between changes in PDRP and PDCP expression over time ($r = 0.81$, P<0.0001), the two network trajectories proved to be different (mean $R^2 = 0.77$ and 0.56 for the PDRP and PDCP, respectively; P<0.04, Wilcoxon signed rank test). This is consistent with the relatively faster increase in PDRP activity that was observed over time. The progressive increases in PDRP expression significantly correlated with concurrent increases in UPDRS motor ratings ($r = 0.62$,

$P<0.005$) and declines in striatal DAT binding (caudate: $r = -0.69$, $P<0.001$; putamen: $r = -0.56$, $P<0.01$). Longitudinal changes in PDCP expression did not correlate with advancing motor disability or with concurrent changes in striatal DAT binding.

Effect of initial treatment

At baseline, there were no significant differences between treated and drug-naïve patients in PDRP/PDCP expression or caudate/putamen DAT binding ($P>0.19$). However, the baseline medicated subjects exhibited lower off-state UPDRS motor ratings than their drug-naïve counterparts ($P<0.02$). Two-way RMANOVA revealed no significant main effect of initial treatment status ($P>0.27$) and no interaction effect of initial medication status and time ($P>0.14$) for the UPDRS motor ratings, caudate/putamen DAT binding and PDRP/PDCP network activity. Thus, rates of progression in these measures are similar for drug-naïve and initially treated patients.

Discussion

In this longitudinal PET study, we found that early stage PD is associated with progressive changes in regional metabolism at key nodes of the two functional brain networks that characterize this disorder. Increasing regional metabolism was observed within elements of the motor-related PDRP network, which evolved in parallel with deterioration in striatal DAT binding and UPDRS motor ratings. In contrast, the declines in cortical metabolism that were seen with advancing disease were associated with changes in the activity of the cognition-related PDCP network. Significant elevations in PDCP activity occurred late in the follow-up period, and did not correlate with motor ratings or with dopaminergic imaging measures of disease progression. These findings indicate that the functioning of motor- and cognition-related neural systems is dissociated at the earliest symptomatic phases of the disease.

Changes in glucose metabolism with disease progression

A whole-brain search of the longitudinal FDG PET data revealed progressive increases in the metabolic activity of the STN, GPi, PPN and motor cortex, regions that have been demonstrated experimentally to mediate the motor manifestations of parkinsonism (Parent and Hazrati, 1995; Middleton and Strick, 2000; Wichman and DeLong, 2003). In contrast, declining metabolic activity was observed in prefrontal and parietal association cortex, areas associated with cognitive dysfunction in this disorder (Huang *et al*., 2007; see Carbon and Marié, 2003 for review).

The role of the STN in the pathophysiology of PD and its treatment has been reviewed elsewhere (Hamani *et al*., 2004; cf. Asanuma *et al*., 2006; Trošt *et al*., 2006). Increased neural activity in the STN is a consistent feature of both clinical and experimental parkinsonism. Nonetheless, regional glucose metabolism has been found to be reduced in this region when measured in animal models (Palombo *et al*., 1990; Carlson *et al*., 1999). Regional glucose utilization predominantly reflects local synaptic activity and the biochemical maintenance processes of the rest state (Jueptner and Weiller, 1995; Eidelberg *et al*., 1997). Therefore, the decline in STN metabolism in experimental parkinsonism has

been viewed as a consequence of a reduction in inhibitory afferents from the external pallidum. However, other lines of evidence have pointed to an increase in STN metabolic activity in parkinsonism (Hirsch *et al*., 2000), attributed to overactivity of excitatory projections to this region from the PPN, intralaminar thalamus and the motor cortex (cf. Parent and Hazrati, 1995). Our observation of steady increases in STN metabolism with advancing disease supports the latter notion. In this vein, the progressive increases in GPi metabolism that were also observed in the current study are likely the consequence of increased STN output to this area. Although these pallidal increases were discerned in the rest state, they appear to correlate with changes in the neural activity of this region during movement. Indeed, we have recently reported progressive increases in pallidal activation during the performance of a motor task that was kinematically controlled across the first two timepoints (Carbon *et al*., 2007).

It is noteworthy that the primary motor cortex and the PPN, two prominent sources of excitatory input to STN, also exhibited increases in glucose utilization with advancing disease. Hypersynchrony of motor cortical neuronal activity has been observed as a prominent feature of nigral dopamine depletion in parkinsonian primates (Goldberg *et al*., 2002). This phenomenon may be the basis for the localized increases in metabolism in this region that we have observed in untreated PD patients (Asanuma *et al*., 2006). The time course data indicated that metabolic increases in the motor cortex reached significance with respect to healthy control values at the second timepoint, while in the STN regional metabolism attained an abnormal level only at the end of the study. This is consistent with the notion that in parkinsonism, the STN functions as a modulator of this cortically generated synchronous high-frequency oscillation (Levy *et al*., 2002).

Unlike the other regions with increasing glucose consumption in the course of disease progression, regional metabolism in the primary motor cortex and SMA did not rise continuously over time (see Fig. 4B, *middle right panel*). Rather, metabolic activity in this region rose initially and then remained stable at an elevated value relative to the healthy controls. Interestingly, these changes were more closely associated with concurrent UPDRS tremor ratings ($r = 0.73$, $P<0.001$; Bland–Altman correlation coefficient) than those occurring in the other regions with longitudinal increases in metabolic activity ($r = 0.49$, 0.48 and 0.32 for the PPN, STN and GPi, respectively). We note that tremor ratings in our subjects also reached an early plateau (mean ± SE: 0.4 ± 0.2; 1.9 ± 0.8; 2.2 ± 0.6 for the three timepoints). It is therefore likely that the metabolic changes in the primary motor cortex/SMA reflected progression in this specific disease manifestation.

The origin of the progressive metabolic increases in the PPN is less clear. Similar changes have been observed in both primate and rodent models of parkinsonism (Palombo *et al*., 1990; Carlson *et al*., 1999), and have been attributed to overactive input to this structure from the globus pallidus/substantia nigra pars reticularis (SNr), or from the STN. It is interesting however, that the PPN was the only progressively increasing brain region in which glucose metabolism was abnormal at baseline, while in GPi and STN, metabolism reached supernormal levels only at subsequent timepoints. Indeed, it is possible that this early change in PPN metabolic activity is a compensatory response to nigral disease by which dopamine release in the striatum is enhanced (Blaha and Winn, 1993). In contrast,

such an early metabolic effect is not present in the STN to support a compensatory role for this structure in the presymptomatic period (cf. Bezard *et al*., 2003). Although ventral thalamic metabolic activity has been found to correlate consistently with spontaneous GPi firing rates in PD patients (Eidelberg *et al*., 1997), firm physiological inferences cannot always be made based upon *in vivo* metabolic measurements. Conclusions regarding the localization and time course of potential compensatory responses in PD patients will require the assessment of early and late changes in metabolic activity in the hemispheres ipsilateral and contralateral to the initially affected body side.

Our voxel-based approach also revealed several areas in which metabolic activity declined significantly with advancing disease. These regions, the prefrontal cortex and inferior parietal lobule, are involved mainly in cognitive functioning and metabolic reductions, and both areas have been found to correlate with impaired memory and executive function in non-demented PD patients (Huang *et al*., 2007; cf. Carbon and Marié, 2003). Also relevant is that despite highly significant progressive declines over time, metabolic activity in these regions declined to only marginally abnormal levels by the end of the study. This is consistent with the early, mild disease that typified our patients. Indeed, although serial psychometric testing was not performed in this study, there was no gross indication of cognitive impairment in these subjects. Nonetheless, the continuous decline in neural function that was observed in these regions is compatible with an evolving cortically based neurodegenerative process, the histopathological basis for which is currently unknown (see Emre, 2004; Braak *et al*., 2005; cf. Huang *et al*., 2007). Alternatively, these focal metabolic changes may reflect alterations in the activity of cognition-related neural networks involving these brain areas (cf. Carbon *et al*., 2003*b*; 2004).

Development of abnormal network activity

In addition to identifying areas with progressively increasing or decreasing metabolism in early stage PD, we assessed longitudinal changes in the activity of functional networks associated with this disorder. Although motor signs were comparatively mild in our patient cohort, PDRP activity was abnormally elevated throughout the period of observation, even at the initial timepoint. Thus, despite a paucity of regional abnormalities at baseline (see earlier), functional connectivity within motor pathways is likely to have been altered by this time.

In previous studies, we have consistently found that PDRP scores correlate with clinical severity ratings (e.g. Eidelberg *et al*., 1995; Feigin *et al*., 2002; Lozza *et al*., 2004; Asanuma *et al*., 2006). Thus, it is not surprising that network activity in individual patients increased over time and correlated with concurrent measures of disease progression obtained by clinical assessment and by dopaminergic imaging. Specifically, longitudinal changes in PDRP expression were associated with increases in motor UPDRS ratings and declines in striatal DAT binding. Although these indices of disease progression were inter-correlated, no more than 40% of their variability was shared between any two of them. Thus, these progression measures are not interchangeable; each one is likely to provide unique information concerning the disease process. We also note that although PDRP activity is reduced by effective antiparkinsonian therapy (e.g. Asanuma *et al*., 2006; cf. Eckert and

Eidelberg, 2005), the 12-h medication washout that was used in this study was adequate for the assessment of progression with this measure. In other words, our data suggest that the influence of disease progression on PDRP expression outweighs the residual effects on network activity that may be present following incomplete washout. Rigorous washout studies of chronically treated patients will be needed to determine the time course of these residual effects on network activity.

PDCP scores also increased with advancing disease, correlating significantly with concurrent changes in PDRP expression. Nonetheless, the trajectories of the two networks over time were different, with significant increases in the former becoming evident only between the second and third timepoints. Indeed, PDCP activity reached abnormal levels only at the final timepoint, whereas PDRP activity was abnormal at baseline. It is conceivable that the relatively late increase in PDCP expression observed in this study is a reflection of incipient cognitive impairment (cf. Huang *et al*., in press). Further follow-up with serial psychometrics and network quantification will be needed to explore this possibility. In any event, the distinctive trajectories of the two PD-related networks suggest that discrete pathophysiological mechanisms underlie the motor and cognitive features of the disease. This notion is further supported by the dissociation of these patterns in response to antiparkinsonian therapy (Asanuma *et al*., 2006; Huang *et al*., 2007). These findings suggest a role for FDG PET imaging in monitoring both motor and cognitive features of disease progression.

Relationship to clinical and dopaminergic progression measures

In this study, we also measured longitudinal changes in UPDRS motor ratings and striatal DAT binding. Our findings accord with the results of other studies in which rates of disease progression were assessed using the UPDRS, striatal DAT binding indices or both. In our cohort, off-state motor ratings deteriorated at a rate of 2.1 points per year, which was comparable to the findings of other prospective imaging studies (Hilker *et al*., 2002; cf. Parkinson-Study-Group, 1993). While our regression-based estimate was consistent with a linear process, the rise in the motor ratings was comparatively steeper during the first 2 years of the study. We note that this rate, approximating 3 points per year, is slower than that reported for placebo-treated patients in a recent clinical trial of the effects of levodopa on disease progression (Fahn *et al*., 2004). We attribute this difference to the younger age of onset and longer duration of symptoms in our study (Jankovic and Kapadia, 2001; Alves *et al*., 2005). This suggests that slowing in the rate of clinical deterioration may occur with advancing disease.

Likewise, the decline in striatal DAT binding in our cohort was in line with other longitudinal PET studies in PD employing this measure of presynaptic nigrostriatal function (see Au *et al*., 2005 for review). Our estimates of loss in striatal binding resembled those measured with 2β-carbomethoxy-3β-(4-[^{18}F]-fluorophenyl)tropane ([^{18}F]-CFT), another radioflourinated PET ligand for quantifying DAT binding (Nurmi *et al*., 2003). We note that in the prior study, all patients were drug-naïve at baseline and that levodopa therapy was initiated in nearly all during the follow-up period. Similarly, in our study, all the initially untreated participants required levodopa by the time of the final imaging session. It has been

suggested based upon the results of the recent ELLDOPA trial (Fahn *et al*., 2004) that chronic levodopa therapy can reduce estimates of striatal DAT binding obtained with radiotracer-based imaging (cf. Ravina *et al*., 2005). Therefore, it is conceivable that the decline in this measure observed in longitudinal studies of initially untreated subjects may be a reflection of this pharmacological effect, rather than of true disease progression. Nonetheless, the presence of a significant negative correlation between changes in caudate/putamen DAT binding and motor UPDRS ratings argues against this possibility. Indeed, our findings are consistent with the results of previous cross-sectional studies in which correlations of similar magnitude (R^2 ~ 35%) were reported between these measures of disease progression (Seibyl *et al*., 1995; Asenbaum *et al*., 1997; Kazumata *et al*., 1998). Thus, as with PDRP, imaging descriptors of dopaminergic dysfunction correlate with motor disability ratings, but not to a degree that would make one or the other measure redundant.

As with the clinical ratings, the serial assessments of striatal DAT binding that were obtained were consistent with a linear process. Interestingly, the decline in putamen DAT binding between the first and final visits correlated significantly with baseline values (R^2 = 0.87, P<0.0005). We note that the presence of such a correlation is typically indicative of a non-linear process (e.g. Hilker *et al*., 2005), which would explain the relatively greater rate of DAT binding loss seen in the caudate and the ipsilateral putamen. However, at this stage of disease, the between-subject variability in putamen DAT binding was relatively small, with progressive declines in the coefficient of variation (COV) over time (see Table 1 and error bars in Fig. 3). Thus, individual differences in baseline binding values were perhaps less likely to influence the rate of change than at earlier disease stages. In other words, our study was conducted at a time in the disease process when between-subject variability was declining, while the within-subject rate of change was relatively constant. This scenario is compatible with an incipient floor effect. In contrast, during the same time period, there was only minimal decline in COV for caudate DAT binding. The absence of an observed floor effect on the caudate measure may explain why the correlation with PDRP change was stronger for DAT binding decrements in this region relative to the putamen. Longer term assessment of these patients with FP-CIT PET will help determine whether such an effect is truly present in our data.

Although the number of patients followed in our study was comparatively small, the progression data were overall quite robust. Nonetheless, certain aspects of the findings will require further validation. Specifically, we found that baseline UPDRS motor ratings were significantly lower in the seven participants who were on chronic antiparkinsonian therapy at the time of enrollment. Six of these subjects were treated with selegiline and/or dopamine agonists, of whom three were also on levodopa. Thus, residual central effects of any of these medications could account for the lower degree of disability that was observed at baseline, even following a 12-h washout.

Despite this difference in baseline motor ratings, comparable effects were not observed in the imaging measures. Thus, in this limited, heterogenous treatment cohort, there was no effect of initial treatment status on baseline measures of striatal DAT binding or PDRP expression. Nonetheless, as discussed above, subtle effects of chronic therapy on either measure cannot be excluded (cf. Fahn *et al*., 2004). Our data also suggest that initial

treatment status did not influence subsequent disease progression, whether assessed clinically or by imaging. Although based on a relatively small number of subjects, this observation is consistent with a recent study of the long-term UPDRS data collected in neuroprotection trials (Guimaraes *et al*., 2005). Additionally, despite the major changes in medication regimen that occurred in the course of the study, the presence of consistent correlations between the progression indices suggests that chronic treatment did not selectively influence any one of these measures. Indeed, it appears that these biomarkers are more sensitive to disease progression than to residual treatment effects that might persist following a 12-h washout. Further studies will be needed to determine the optimal period of washout needed to minimize this potential confound.

Acknowledgments

This work was supported by NIH NINDS R01 35069, P50 NS 38370 and by the General Clinical Research Center of the North Shore-Long Island Jewish Health System (M01 RR 018535). P50 NS 38370. The authors wish to thank Dr Thomas Chaly for radiochemistry support and Mr Claude Margouleff for technical assistance in performing the PET studies. Special thanks to Ms Shivani Rachakonda for data management and Ms Toni Flanagan for valuable editorial assistance.

Abbreviations

SPM	statistical parametric mapping
FDR	false discovery rate
STN	subthalamic nucleus

References

Alves G, Wentzel-Larsen T, Aarsland D, Larsen JP. Progression of motor impairment and disability in Parkinson disease: a population-based study. Neurology. 2005; 65:1436–41. [PubMed: 16275832]

Alves G, Larsen JP, Emre M, Wentzel-Larsen T, Aarsland D. Changes in motor subtype and risk for incident dementia in Parkinson's disease. Mov Disord. 2006; 21:1123–30. [PubMed: 16637023]

Asanuma K, Ma Y, Huang C, Carbon-Correll M, Edwards C, Raymond D, et al. The metabolic pathology of dopa-responsive dystonia. Ann Neurol. 2005; 57:596–600. [PubMed: 15786454]

Asanuma K, Tang C, Ma Y, Dhawan V, Mattis P, Edwards C, et al. Network modulation in the treatment of Parkinson's disease. Brain. 2006; 129 (Pt 10):2667–78. [PubMed: 16844713]

Asenbaum S, Brucke T, Pirker W, Podreka I, Angelberger P, Wenger S, et al. Imaging of dopamine transporters with iodine-123-beta-CIT and SPECT in Parkinson's disease. J Nucl Med. 1997; 38:1–6. [PubMed: 8998140]

Au WL, Adams JR, Troiano AR, Stoessl AJ. Parkinson's disease: in vivo assessment of disease progression using positron emission tomography. Brain Res Mol Brain Res. 2005; 134:24–33. [PubMed: 15790527]

Bezard E, Gross CE, Brotchie JM. Presymptomatic compensation in Parkinson's disease is not dopamine-mediated. Trends Neurosci. 2003; 26:215–21. [PubMed: 12689773]

Blaha CD, Winn P. Modulation of dopamine efflux in the striatum following cholinergic stimulation of the substantia nigra in intact and pedunculopontine tegmental nucleus-lesioned rats. J Neurosci. 1993; 13:1035–44. [PubMed: 8441002]

Bland JM, Altman DG. Calculating correlation coefficients with repeated observations: Part 1–Correlation within subjects. Br Med J. 1995; 310:446. [PubMed: 7873953]

Braak H, Rub U, Jansen Steur EN, Del Tredici K, de Vos RA. Cognitive status correlates with neuropathologic stage in Parkinson disease. Neurology. 2005; 64:1404–10. [PubMed: 15851731]

Brooks DJ, Frey KA, Marek KL, Oakes D, Paty D, Prentice R, et al. Assessment of neuroimaging techniques as biomarkers of the progression of Parkinson's disease. Exp Neurol. 2003; 184 (Suppl 1):S68–79. [PubMed: 14597329]

Carbon M, Marié RM. Functional imaging of cognition in Parkinson's disease. Curr Opin Neurol. 2003; 16:475–80. [PubMed: 12869806]

Carbon M, Edwards C, Eidelberg D. Functional brain imaging in Parkinson's disease. Adv Neurol. 2003a; 91:175–81. [PubMed: 12442676]

Carbon M, Ghilardi MF, Dhawan V, Eidelberg D. Correlates of movement initiation and velocity in Parkinson's disease: a longitudinal PET study. Neuroimage. 2007; 34:361–70. [PubMed: 17064939]

Carbon M, Ma Y, Barnes A, Dhawan V, Chaly T, Ghilardi MF, et al. Caudate nucleus: influence of dopaminergic input on sequence learning and brain activation in parkinsonism. Neuroimage. 2004; 21:1497–507. [PubMed: 15050574]

Carbon M, Ghilardi MF, Feigin A, Fukuda M, Nakamura T, Dhawan V, et al. Learning networks in health and Parkinson's disease: reproducibility and treatment effects. Hum Brain Mapp. 2003b; 19:197–211. [PubMed: 12811735]

Carlson JD, Pearlstein RD, Buchholz J, Iacono RP, Maeda G. Regional metabolic changes in the pedunculopontine nucleus of unilateral 6-hydroxydopamine Parkinson's model rats. Brain Res. 1999; 828:12–9. [PubMed: 10320720]

Eckert T, Eidelberg D. Neuroimaging and therapeutics in movement disorders. Neurorx. 2005; 2:361–71. [PubMed: 15897956]

Eckert T, Van Laere K, Tang C, Lewis DE, Edwards C, Santens P, et al. Quantification of PD-related network expression with ECD SPECT. Eur J Nucl Med Mol Imaging. 2007; 34:495–501.

Eidelberg D, Moeller JR, Ishikawa T, Dhawan V, Spetsieris P, Chaly T, et al. Assessment of disease severity in parkinsonism with fluorine-18-fluorodeoxyglucose and PET. J Nucl Med. 1995; 36:378–83. [PubMed: 7884498]

Eidelberg D, Moeller JR, Dhawan V, Spetsieris P, Takikawa S, Ishikawa T, et al. The metabolic topography of parkinsonism. J Cereb Blood Flow Metab. 1994; 14:783–801. [PubMed: 8063874]

Eidelberg D, Moeller JR, Kazumata K, Antonini A, Sterio D, Dhawan V, et al. Metabolic correlates of pallidal neuronal activity in Parkinson's disease. Brain. 1997; 120:1315–24. [PubMed: 9278625]

Ellis SP, Underwood MD, Arango V, Mann JJ. Mixed models and multiple comparisons in analysis of human neurochemical maps. Psychiatry Res. 2000; 99:111–9. [PubMed: 10963986]

Emre M. Dementia in Parkinson's disease: cause and treatment. Curr Opin Neurol. 2004; 17:399–404. [PubMed: 15247534]

Fahn, S.; Elton, R. Commitee atmotUPsDRSD. Unified Parkinson's Disease Rating Scale. In: Fahn, S.; Marsden, CD.; Calne, D., editors. Recent developments in Parkinson's disease. New York: MacMillan; 1987. p. 153-63.

Fahn S, Oakes D, Shoulson I, Kieburtz K, Rudolph A, Lang A, et al. Levodopa and the progression of Parkinson's disease. N Engl J Med. 2004; 351:2498–508. [PubMed: 15590952]

Fearnley JM, Lees AJ. Ageing and Parkinson's disease: substantia nigra regional selectivity. Brain. 1991; 114 (Pt 5):2283–301. [PubMed: 1933245]

Feigin A, Antonini A, Fukuda M, De Notaris R, Benti R, Pezzoli G, et al. Tc-99m ethylene cysteinate dimer SPECT in the differential diagnosis of parkinsonism. Mov Disord. 2002; 17:1265–70. [PubMed: 12465066]

Goldberg JA, Boraud T, Maraton S, Haber SN, Vaadia E, Bergman H. Enhanced synchrony among primary motor cortex neurons in the 1-methyl-4-phenyl-1,2,3,6-tetrahydropyridine primate model of Parkinson's disease. J Neurosci. 2002; 22:4639–53. [PubMed: 12040070]

Guimaraes P, Kieburtz K, Goetz CG, Elm JJ, Palesch YY, Huang P, et al. Non-linearity of Parkinson's disease progression: implications for sample size calculations in clinical trials. Clin Trials. 2005; 2:509–18. [PubMed: 16422311]

Hamani C, Saint-Cyr JA, Fraser J, Kaplitt M, Lozano AM. The subthalamic nucleus in the context of movement disorders. Brain. 2004; 127:4–20. [PubMed: 14607789]

Hilker R, Voges J, Thiel A, Ghaemi M, Herholz K, Sturm V, et al. Deep brain stimulation of the subthalamic nucleus versus levodopa challenge in Parkinson's disease: measuring the on- and off-conditions with FDG-PET. J Neural Transm. 2002; 109:1257–64. [PubMed: 12373559]

Hilker R, Schweitzer K, Coburger S, Ghaemi M, Weisenbach S, Jacobs AH, et al. Nonlinear progression of Parkinson disease as determined by serial positron emission tomographic imaging of striatal fluorodopa F 18 activity. Arch Neurol. 2005; 62:378–82. [PubMed: 15767502]

Hilker R, Voges J, Ghaemi M, Lehrke R, Rudolf J, Koulousakis A, et al. Deep brain stimulation of the subthalamic nucleus does not increase the striatal dopamine concentration in parkinsonian humans. Mov Disord. 2003; 18:41–8. [PubMed: 12518299]

Hirsch EC, Perier C, Orieux G, Francois C, Feger J, Yelnik J, et al. Metabolic effects of nigrostriatal denervation in basal ganglia. Trends Neurosci. 2000; 23:S78–85. [PubMed: 11052224]

Huang C, Mattis P, Julin P. Identifying functional imaging markers of mild cognitive impairment in early Alzheimer's and Parkinson's disease using multivariate analysis. Clin Neurosci Res. (in press).

Huang C, Mattis P, Tang C, Perrine K, Carbon M, Eidelberg D. Metabolic brain networks associated with cognitive function in Parkinson's disease. Neuroimage. 2007; 34:714–23. [PubMed: 17113310]

Hughes AJ, Daniel SE, Kilford L, Lees AJ. Accuracy of clinical diagnosis of idiopathic Parkinson's disease: a clinico-pathological study of 100 cases. J Neurol Neurosurg Psychiatry. 1992; 55:181–4. [PubMed: 1564476]

Jankovic J, Kapadia AS. Functional decline in Parkinson disease. Arch Neurol. 2001; 58:1611–5. [PubMed: 11594919]

Jueptner M, Weiller C. Review: does measurement of regional cerebral blood flow reflect synaptic activity? Implications for PET and fMRI. Neuroimage. 1995; 2:148–56. [PubMed: 9343597]

Kazumata K, Dhawan V, Chaly T, Antonini A, Margouleff C, Belakhlef A, et al. Dopamine transporter imaging with fluorine-18-FPCIT and PET. J Nucl Med. 1998; 39:1521–30. [PubMed: 9744335]

Levy R, Ashby P, Hutchison WD, Lang AE, Lozano AM, Dostrovsky JO. Dependence of subthalamic nucleus oscillations on movement and dopamine in Parkinson's disease. Brain. 2002; 125:1196–209. [PubMed: 12023310]

Lozza C, Baron JC, Eidelberg D, Mentis MJ, Carbon M, Marie RM. Executive processes in Parkinson's disease: FDG-PET and network analysis. Hum Brain Mapp. 2004; 22:236–45. [PubMed: 15195290]

Ma Y, Tang C, Spetsieres P, Dhawan V, Eidelberg D. Abnormal metabolic network activity in Parkinson's disease: Test-retest reproducibility. J Cereb Blood Flow Metab. 2007; 27:501–509. [PubMed: 16835631]

Ma Y, Dhawan V, Mentis M, Chaly T, Spetsieris PG, Eidelberg D. Parametric mapping of [18F]FPCIT binding in early stage Parkinson's disease: a PET study. Synapse. 2002; 45:125–33. [PubMed: 12112405]

Marek K, Jennings D, Seibyl J. Dopamine agonists and Parkinson's disease progression: what can we learn from neuroimaging studies. Ann Neurol. 2003; 53:S160–6. [PubMed: 12666107]

Mentis MJ, McIntosh AR, Perrine K, Dhawan V, Berlin B, Feigin A, et al. Relationships among the metabolic patterns that correlate with mnemonic, visuospatial, and mood symptoms in Parkinson's disease. Am J Psychiatry. 2002; 159:746–54. [PubMed: 11986127]

Middleton FA, Strick PL. Basal ganglia and cerebellar loops: motor and cognitive circuits. Brain Res Brain Res Rev. 2000; 31:236–50. [PubMed: 10719151]

Moeller JR, Eidelberg D. Divergent expression of regional metabolic topographies in Parkinson's disease and normal ageing. Brain. 1997; 120:2197–206. [PubMed: 9448575]

Moeller JR, Nakamura T, Mentis MJ, Dhawan V, Spetsieres P, Antonini A, et al. Reproducibility of regional metabolic covariance patterns: comparison of four populations. J Nucl Med. 1999; 40:1264–9. [PubMed: 10450676]

Morrish PK, Rakshi JS, Bailey DL, Sawle GV, Brooks DJ. Measuring the rate of progression and estimating the preclinical period of Parkinson's disease with [18F]dopa PET. J Neurol Neurosurg Psychiatry. 1998; 64:314–9. [PubMed: 9527140]

Nakamura T, Dhawan V, Chaly T, Fukuda M, Ma Y, Breeze R, et al. Blinded positron emission tomography study of dopamine cell implantation for Parkinson's disease. Ann Neurol. 2001; 50:181–7. [PubMed: 11506400]

Nurmi E, Bergman J, Eskola O, Solin O, Vahlberg T, Sonninen P, et al. Progression of dopaminergic hypofunction in striatal subregions in Parkinson's disease using [18F]CFT PET. Synapse. 2003; 48:109–15. [PubMed: 12645035]

Palombo E, Porrino LJ, Bankiewicz KS, Crane AM, Sokoloff L, Kopin IJ. Local cerebral glucose utilization in monkeys with hemiparkinsonism induced by intracarotid infusion of the neurotoxin MPTP. J Neurosci. 1990; 10:860–9. [PubMed: 2319306]

Parent A, Hazrati LN. Functional anatomy of the basal ganglia. I. The cortico-basal ganglia-thalamo-cortical loop. Brain Res Brain Res Rev. 1995; 20:91–127. [PubMed: 7711769]

Parkinson-Study-Group. Effects of tocopherol and deprenyl on the progression of disability in early Parkinson's disease. The Parkinson Study Group. N Engl J Med. 1993; 328:176–83. [PubMed: 8417384]

Ravina B, Eidelberg D, Ahlskog JE, Albin RL, Brooks DJ, Carbon M, et al. The role of radiotracer imaging in Parkinson disease. Neurology. 2005; 64:208–15. [PubMed: 15668415]

Schmahmann, JD.; Doyon, J.; Toga, AW.; Petrides, M.; Evans, AC. MRI atlas of the human cerebellum. San Diego: Academic Press; 2000.

Searle, SS.; Casella, G.; McCulloch, CE. Variance components. New York: John Wiley & Sons; 1992.

Seibyl JP, Marek KL, Quinlan D, Sheff K, Zoghbi S, Zea-Ponce Y, et al. Decreased single-photon emission computed tomographic [123I]beta-CIT striatal uptake correlates with symptom severity in Parkinson's disease. Ann Neurol. 1995; 38:589–98. [PubMed: 7574455]

Spetsieris P, Ma Y, Dhawan V, Moeller JR, Eidelberg D. Highly automated computer-aided diagnosis of neurological disorders using functional brain imaging. Proc SPIE: Med Imaging. 2006; 6144:61445M1–12.

Takikawa S, Dhawan V, Spetsieris P, Robeson W, Chaly T, Dahl R, et al. Noninvasive quantitative fluorodeoxyglucose PET studies with an estimated input function derived from a population-based arterial blood curve. Radiology. 1993; 188:131–6. [PubMed: 8511286]

Trošt M, Su S, Su PC, Yen R-F, Tseng H-M, Barnes A, et al. Network modulation by the subthalamic nucleus in the treatment of Parkinson's disease. Neuroimage. 2006; 31:301–07. [PubMed: 16466936]

Whone AL, Watts RL, Stoessl AJ, Davis M, Reske S, Nahmias C, et al. Slower progression of Parkinson's disease with ropinirole versus levodopa: The REAL-PET study. Ann Neurol. 2003; 54:93–101. [PubMed: 12838524]

Wichman T, DeLong MR. Pathophysiology of Parkinson's disease: the MPTP primate model of the human disorder. Ann NY Acad Sci. 2003; 991:199–213. [PubMed: 12846988]

Zetusky WJ, Jankovic J, Pirozzolo FJ. The heterogeneity of Parkinson's disease: clinical and prognostic implications. Neurology. 1985; 35:522–6. [PubMed: 3982637]

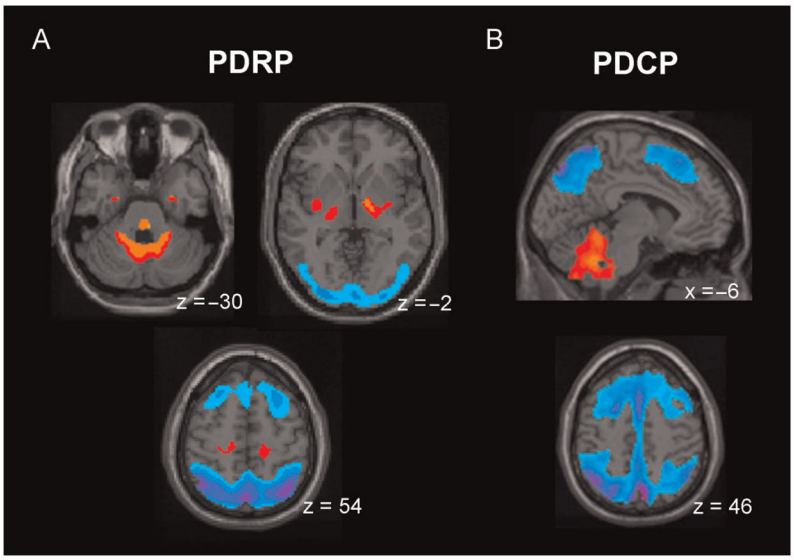

Fig. 1.

Parkinson's Disease-Related Spatial Covariance Patterns. **(A)** Parkinson's Disease-Related Pattern (PDRP). This motor-related metabolic pattern was identified by network analysis of [^{18}F]-fluorodeoxyglucose (FDG) positron emission tomography (PET) scans from 33 PD patients and 33 age-matched healthy volunteers (Ma *et al*., 2007). This pattern was characterized by relative increases in pallidothalamic, pontocerebellar and motor cortical/supplementary motor area (SMA) metabolic activity (*top*), associated with reductions in the lateral premotor and posterior parietal areas (*bottom*). PDRP expression was significantly increased in the PD cohort (P<0.001) compared to controls. **(B)** Parkinson's Disease-Related Cognitive Pattern (PDCP). This cognition-related metabolic pattern was identified in the network analysis of FDG PET scans from 15 non-demented PD patients with mild-moderate motor symptoms (Huang *et al*., 2007). This pattern was characterized by relative hypometabolism of dorsolateral prefrontal cortex, rostral supplementary motor area (preSMA) and superior parietal regions, associated with relative cerebellar/dentate nucleus metabolic increases. PDCP expression correlated significantly (P<0.01) with psychometric indices of memory and executive functioning. [The displays represent voxels that contribute significantly (P<0.001) to each of the two networks. Voxels with positive region weights (metabolic increases) are colour-coded from red to yellow; those with negative region weights (metabolic decreases) are colour-coded from blue to purple.]

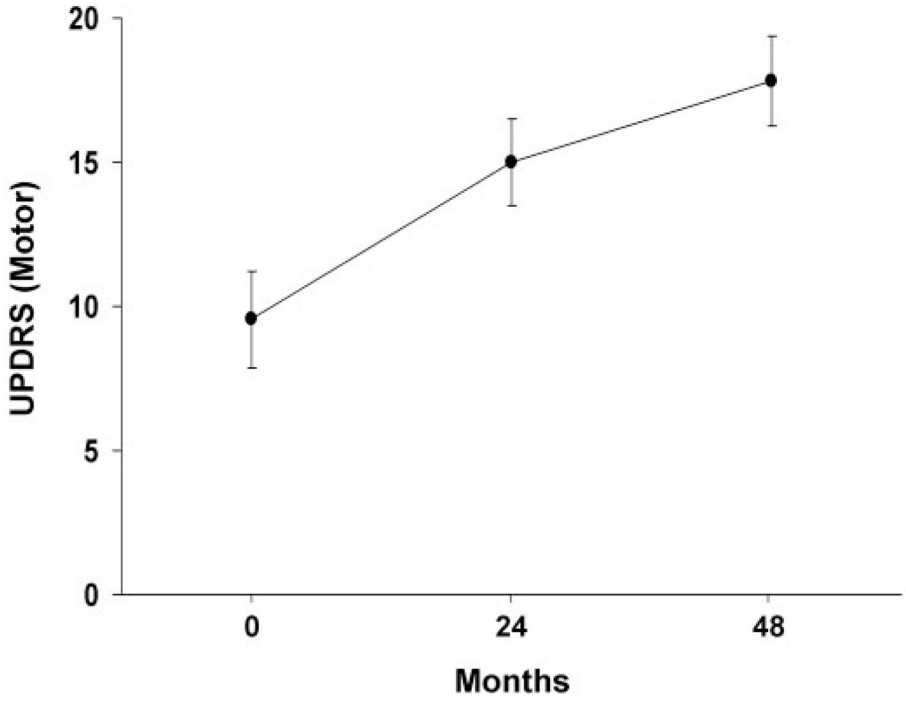

Fig. 2.

Mean off-state Unified Parkinson's Disease Rating Scale (UPDRS) motor ratings at baseline, 24 and 48 months. These scores increased linearly over time ($P<0.0001$; RMANOVA), at a rate of 2.1 units per year (see text). [Bars represent the standard error at each timepoint.]

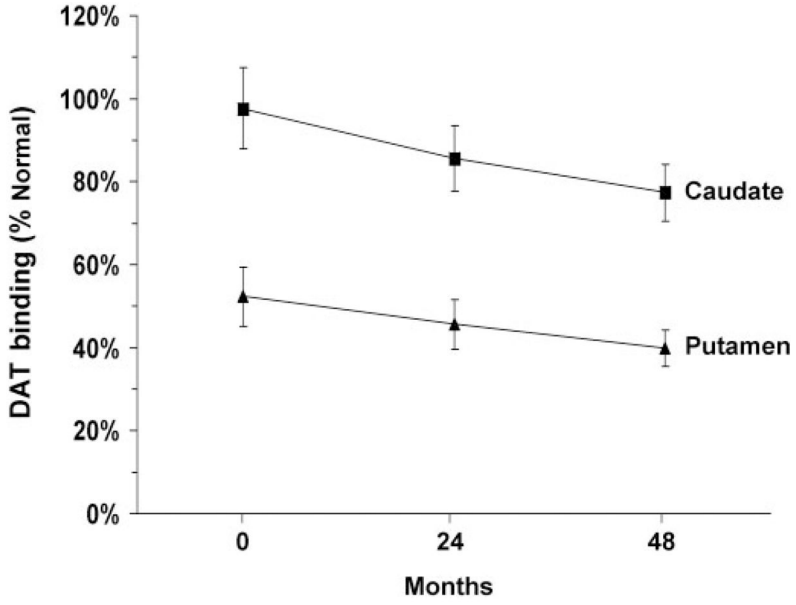

Fig. 3.

Mean striatal DAT binding at baseline, 24 and 48 months. Values for the caudate (*squares*) and putamen (*triangles*) are represented as percent of the normal mean value for each region (see text). In both regions, DAT binding declined linearly over time ($P<0.003$; RMANOVA). [Bars represent the standard error at each timepoint.]

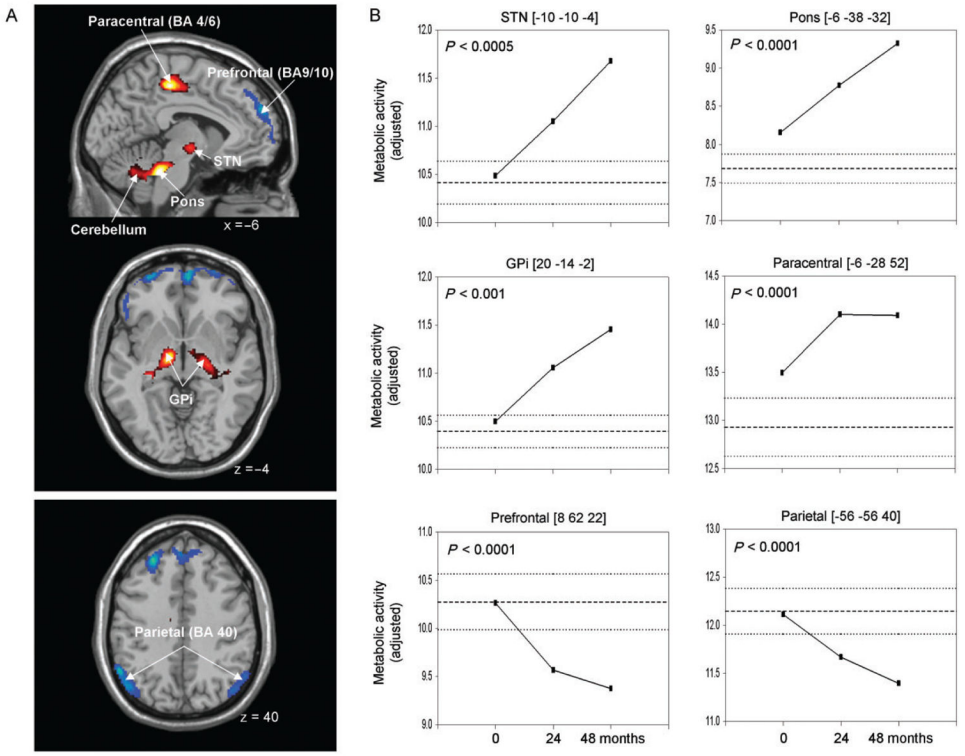

Fig. 4.

(**A**) Voxel-based analysis of longitudinal changes in regional metabolic activity. Metabolic increases with disease progression (*top*) are displayed using a red–yellow scale. Progressive metabolic declines (*bottom*) are displayed using a blue–purple scale. Both displays were superimposed on a single-subject MRI brain template and thresholded at $t = 3.48$, $P = 0.001$ (peak voxel, uncorrected). (**B**) Displays of the metabolic data for these individual regions at each timepoint (Table 2). The significance level (*P*-value) of the repeated measures analysis of variance (RMANOVA) is presented for each region (see text). [The coordinates refer to the Montreal Neurological Institute (MNI) standard space. GPi: internal globus pallidus, STN: subthalamic nucleus, BA: Brodmann area.]

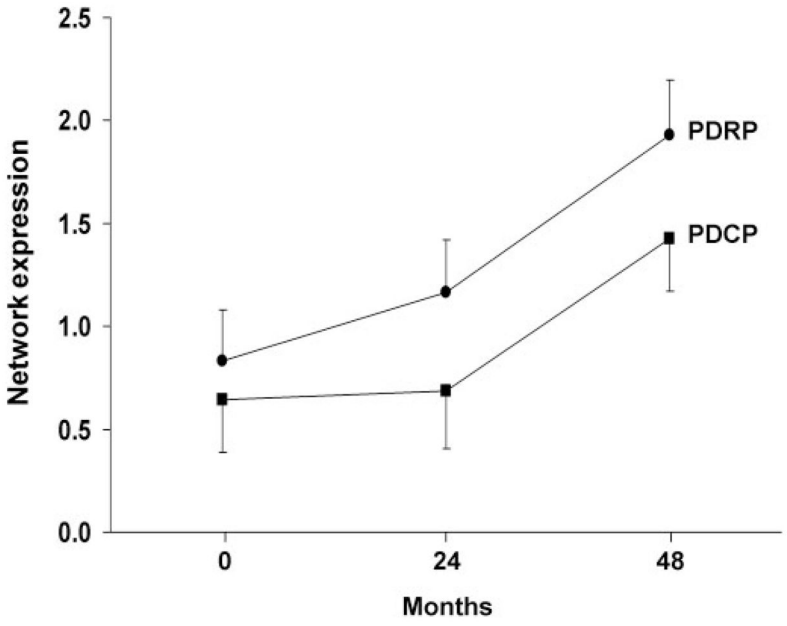

Fig. 5.

Mean network activity at baseline, 24 and 48 months. Values for the PD-related motor and cognitive spatial covariance patterns (PDRP and PDCP; see Fig. 1) were computed at each timepoint and displayed relative to the mean for 15 age-matched healthy subjects (see text). Network activity increased significantly over time for both patterns ($P<0.0001$; RMANOVA), with the PDRP progressing faster than the PDCP ($P<0.04$). Relative to controls, PDRP activity in the patient group was elevated at all three timepoints, while PDCP activity reached abnormal levels only at the final timepoint. [Bars represent the standard error at each timepoint.]

Table 1

Striatal dopamine transporter binding at baseline, 24 and 48 months

	Baseline	24 Months	48 Months	Controls
Caudate	2.69 ± 0.84[a]	2.45 ± 0.66	2.14 ± 0.56*	2.77 ± 0.44
Putamen	1.30 ± 0.51**	1.15 ± 0.44**	0.95 ± 0.32**	2.38 ± 0.29

[a] Mean striato-occipital ratio (SOR) values ± SD (see text).

* $P<0.05$,

** $P<0.001$, compared to age-matched healthy control values (Student's *t*-tests).

Table 2

Regions with significant longitudinal changes in glucose metabolism.

Regions	Coordinates[a]			Z_{max}	*P*-value[c]	Mean adjusted regional glucose metabolism (mg/min/100 g)			
	x	*y*	*z*			Baseline (*n* = 15)	24 Months (*n* = 15)	48 Months (*n* = 10)	Controls (*n* = 15)
Increasing metabolism									
Pons	−6	−38	−32	4.80	<0.001	8.16 ± 0.73*	8.77 ± 0.52***	9.32 ± 0.72***	7.68 ± 0.73
Cerebellum, Lobule VI[b]	30	−60	−46	4.29	<0.001	10.49 ± 0.88	11.02 ± 0.77	11.80 ± 1.00**	10.57 ± 0.91
Paracentral Gyrus (BA 4/6)	−6	−28	52	4.71	<0.001	13.50 ± 0.84	14.10 ± 0.80**	14.09 ± 0.86**	12.93 ± 1.17
Subthalamic nucleus	−10	−10	−4	4.35	0.020	10.49 ± 1.18	11.05 ± 0.90	11.68 ± 1.11**	10.41 ± 0.86
Globus Pallidus (internal)	20	−14	−2	3.85	0.023	10.49 ± 0.97	11.06 ± 0.94**	11.46 ± 1.24*	10.39 ± 0.65
Decreasing metabolism									
Medial Frontal Lobe (BA 9/10)	8	62	22	4.96	<0.001	10.26 ± 0.81	9.57 ± 0.87	9.37 ± 1.09	10.27 ± 1.13
Inferior Parietal Lobule (BA 39/40)	−56	−56	40	4.23	0.008	12.11 ± 0.61	11.67 ± 0.56	11.39 ± 0.56*	12.15 ± 0.92

[a] Montreal Neurological Institute (MNI) standard space; BA = Brodmann Area.

[b] According to the atlas of Schmahmann (Schmahmann et al., 2000).

[c] SPM, *P*-values corrected at the cluster level. All maxima were significant at $P<0.01$, FDR-corrected at the voxel level.

* $P<0.05$,

** $P<0.01$,

*** $P<0.001$, compared to age-matched healthy control values (Student's *t*-tests).